ICCEPM 2024 https://dx.doi.org/10.6106/ICCEPM.2024.0160
The 10th International Conference on Construction Engineering and Project Management
Jul. 29-Aug.1, 2024, Sapporo

Investigation of the Influence of The Story Drift Angle of Buildings Caused by Earthquakes on Elevators

Yuichi ONUMA [1]*, Satoshi FUJITA [2], Osamu FURUYA [3], Yusuke OKI [4], Toshihiro SANKAI[5]

[1] *Graduate School of Advanced Science and Technology, Tokyo Denki University (Visiting Research Engineer, Building Research Institute), Japan,* E-mail address: 22udq02@ms.dendai.ac.jp
[2] *Tokyo Denki University*, *Japan,* E-mail address: sfujita@cck.dendai.ac.jp
[3] *Tokyo Denki University, Japan,* E-mail address: osamu.furuya@mail.dendai.ac.jp
[4] *Building Research Institute, Japan,* E-mail address: oki_y@kenken.go.jp
[5] *National Institute for Land and Infrastructure Management, Japan,* E-mail address: sankai.works@gmail.com

Abstract: In recent years, as buildings have become taller and taller, the continued usability of elevators after earthquakes has become an important issue. Conventional seismic design of elevators has focused mainly on inertial forces caused by earthquakes, but the influence of the story drift angle of buildings on elevator behavior has been unclear. Therefore, the objective of this study was to clarify the influence of the story drift angle of a building caused by an earthquake on the behavior of elevators through an experiment.

The experiment specimens were the counterweight, guide rails, and surrounding components selected from the actual elevator components and mounted on a one-story steel pin frame. A static experiment was conducted using a hydraulic jack to apply force to the specimen by imposing the story drift angle on the steel frame. During the experiment, the reaction force at the end of the jack was monitored, and the displacement and strain of the counterweight, guide rails, and surrounding components were measured.

The results of the experiments in one direction showed that even when the elevator components were subjected to a larger story drift angle than assumed in the seismic design of the building, no damage occurred that could lead to fallout.

Key words: Earthquake Resistance, Elevator, Continued Usability, Static Loading Experiment, Story Drift Angle

1. INTRODUCTION

As buildings become taller and taller, a method of vertical movement such as elevators is becoming more important. The ability of elevators to be restored as quickly as possible after an earthquake and to continue to be used as they would be under normal conditions is considered to have an added value in making buildings resilient to earthquakes. Conversely, risks associated with the continuous use of elevators could threaten the continuity of life for building occupants.

The structural design system for buildings (structural frames) in Japan has been established since 1981, and there are many achievements to date. Methods for predicting the response displacement of buildings are also being used, and it is becoming possible to adopt flexible framing formulas that maintain structural safety even when response displacement is large. On the other hand, elevators are one of the parts (non-structural members) that are not included in the seismic design of the structure, and design regularions are stipulated for each type of elevator.

Among the recent reported elevator stoppage events caused by medium to large earthquakes in Japan, no mention has been made of the direct causes of the effects of building damage. In particular, there are many unexamined and unresolved aspects of events caused by the story drift angles of the building structure, due to earthquakes, and no clear considerations are given in the current regulations. Not enough information for the seismic design between the structure and the elevators has been exchanged. Therefore, it is necessary to consider how to disclose the seismic design considerations of elevators to structural designers.

This paper firstly discusses the overview of the structural design methods for elevator guide rails of the type of rope elevators under the current stipulation. Next, we report on the implementation of an experiment to study the effect of the story drift angle on the counterweight attached to the steel framework and its surrounding components to investigate the effect of the story drift angle in the failure event " de-railing of the counterweight". The behavior of the guide rails is discussed analytically, especially for the consideration of the effect of the story drift angle, and the issues of the verification method based on the current regulations are presented.

2. TECHNICAL STIPULATION FOCUSING ON THE SEISMIC DESIGN OF THE ELEVATOR IN THE BSL IN JAPAN

The strength calculation method for guide rails in the rope elevators under current regulations [1] is shown below.

(1) Calculation model and classification

(i) The calculation model for guide rails is based on a 3-span model.

(ii) The classification is divided into general type cages, counterweights, special counterweights, and building heights of 60 m or less and over 60 m, and the calculation methods are different.

(2) Calculation method (The case of the popular types.)

(i) Building height 60 m or less

・stress intensity: $\sigma = \gamma 1 \times \frac{7}{40} \times \frac{\beta \cdot P \cdot L}{Z}$ (1)

・deflection: $\delta = \gamma 2 \times \frac{11}{960} \times \frac{\beta \cdot P \cdot L^3}{E \cdot I}$ (2)

(ii) Building height over 60m

・stress intensity: $\sigma = \gamma 1 \times \left(\frac{7}{40} \times \frac{\beta \cdot P \cdot L}{Z} + \frac{6 \cdot E \cdot I \cdot \delta'}{5 \cdot L^2 \cdot Z} \right)$ (3)

・deflection: $\delta = \gamma 2 \times \frac{11}{960} \times \frac{\beta \cdot P \cdot L^3}{E \cdot I}$ (4)

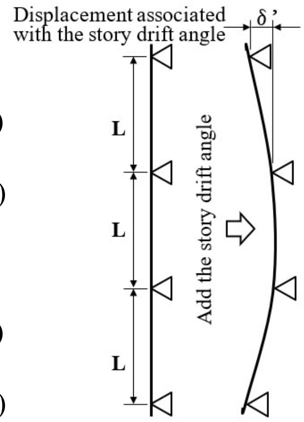

Calculation model (3-span model)

Where P: seismic load, L: rail bracket mounting distance, Z: section modulus of rail, I: rail sectional secondary moment, E: Young's modulus, β: reduction factor, γ1: plate stress coefficient*, γ2: deflection coefficient of the plate*, δ': displacement associated with the story drift angle.

* Guide rails use joint plates with a smaller cross-sectional performance than the guide rail itself at the joints, which may result in higher stress and deflection. Therefore, when calculating rail strength, multiply γ1: stress coefficient of the joint plate and γ2: deflection coefficient of the joint plate, according to the cross-sectional performance of the rail and the joint plate.

As mentioned above, the variation factor due to the story drift angle: δ' is considered only for stress levels at building heights over 60 m, and not for other conditions. In addition, a full-scale elevator vibration test conducted in July 2022 verified the following three factors that may cause confinement when the elevator is running.

(a) De-railing of cage or counterweight

(b) Deformation of the cage (deformation of the cage frame, guide system, etc.)

(c) Open circuit of door-closing switches at the boarding and cage doors

However, we were only able to reproduce (c) the opening paths of the door-closing switches of the boarding and cage doors, and could not reproduce the other cases. It has been reported that one of the reasons for this is that the displacement caused by the story drift angle, such as interference due to the positional relationship between the cage, rail bracket, and landing, could not be simulated. In particular, regarding "(a) De-railing of the cage or counterweight," based on the 3-span model of the current regulations, the deflection is proportional to the cube of L (rail bracket installation interval), so we focus on the rail bracket span, which has the largest influence on the deflection, and the story drift angle is not considered.

3. EXPERIMENTAL APPROACH FOR THE PART OF ELEVATOR APPLIED THE STATIC STORY DRIFT ANGLE OF THE BUILDING

One experiment to introduce the story drift angle into elevator elements is shown as follows. The rope elevator is a system in which the cage and counterweight are supported and balanced by a traction machine (including a deflector sheave) at the top of the elevating track via ropes, but during an earthquake, the counterweight comes into contact with the guide rail that guides the elevator up and down. This paper focuses only on the counterweight and guide rails, referring to the damage "de-railing of the counterweight" in [2].

3.1. Setup and the specimen

Figure 1 shows the setup of the steel frame to simulate the story drift angle of the building experimentally to determine the effect of the story drift angle in the building on the elevator components. The jig has the upper and middle layers. The upper layer is connected to the four columns via pins. An additional beam is attached to the top of the beams on the upper layer. The beam-A in the middle layer (see Figure 1 and Figure 3.) connected to the four columns is joined to a reaction wall via hydraulic jack. Beam-B is pin-connected to columns via beam-B. On the reaction floor, the bottom of the steel frame is joined via pins and the steel base is fixed.

Figure 4 shows an overview of the specimen. The specimen consists of “a rail section” and “a counterweight section”. The rail section consists of two guide rails, each about 3.5 m high, spaced about 750 mm. The guide rails are fastened to steel members (rail brackets) cantilevered from beam-B

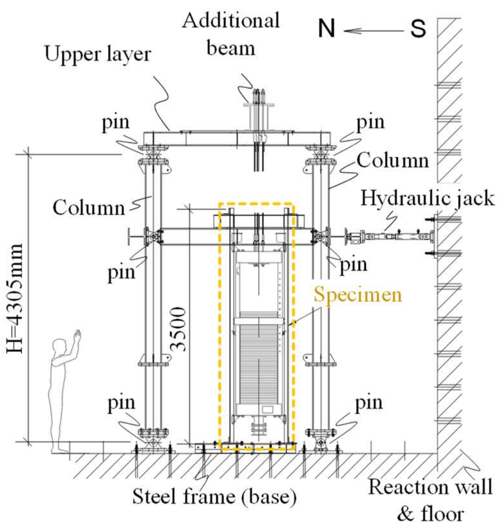

Figure 1. Setup of the steel frame and specimen

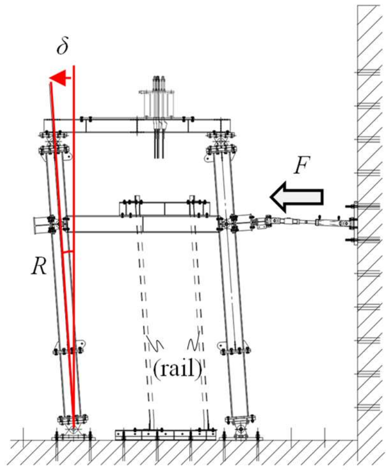

Figure 2. State applied the displacement for story drift angle

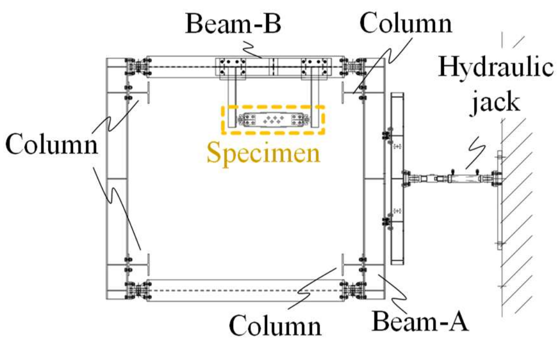

Figure 3. Plan of the middle layer

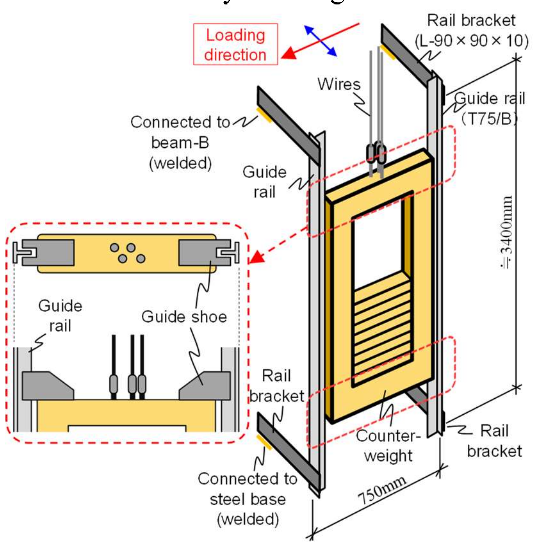

Figure 4. Specimen (a part of the elevator)

for uppermost by parts called rail clips, and are fastened to other rail brackets cantilevered from the steel base for lowermost by them.

In the counterweight section, a counterweight of approximately 1000 kg is supported on the upper beam of the experimental jig via ropes. The counterweight is placed between the two rails at the center height of the guide rails. Components called a guide shoes are installed in the counterweight section at the contact point between the counterweight and the guide rails. These components are shaped to sandwich the guide rails and is installed in two locations per rail (see Figure 3).

3.2. Loading procedure

As shown in Figure 2, the steel frame is entirely tilted by stretching the hydraulic jack and the quasi-static horizontal displacement corresponding to the story drift angle applied to the specimen. The loading conditions are monotonic loading, starting with the frame in an upright position (0% the story drift angle) until the behavior of the counterweight or the rails becomes apparent. The story drift angle is calculated by the following equation,

$$R = \frac{\delta}{H} \times 100 \tag{5}$$

where R is the story drift angle, δ is the horizontal displacement of the upper layer, and H is the distance between the lowest and uppermost pins. This value of R is equivalent to the story drift angle obtained by the horizontal displacement of the middle layer, if the steel frame is appropriately set and no deformation occurs in the steel frame.

3.3. Outline of the experiment results

To confirm the validity of the experimental jig, the force- story drift angle relationship is shown in black lines in Figure 4. Considering the results of the test performed only on the steel frame before the specimen was installed (blue line in Figure 4), the horizontal reaction force was almost negligible.

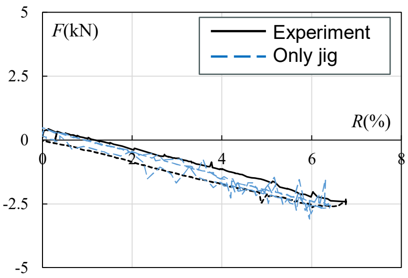

Figure 4. F-R relation

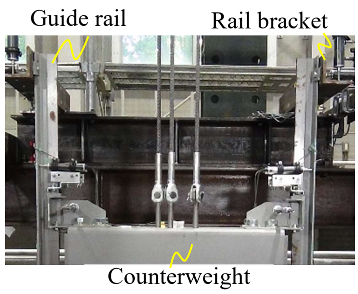

Photo 1(a) neutral state of the story drift

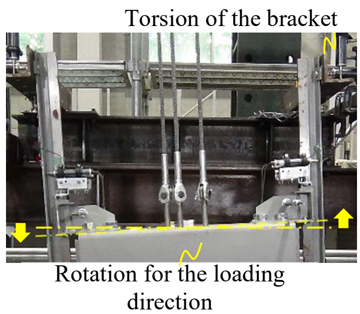

Photo 1(b) state of 6% story drift angle

Photo 1 and Photo 2 show the movement of the counterweight, rail, and the top of the bracket before and after the introduction of the story drift angle. No deformation or damage to the rails was visually observed. In the bracket, it was observed that the cross section was torsion-ally rotated. The counterweights also rotated as the story drift angle was introduced. The deformation of the counterweight's frame material itself was very small relative to rotation.

3.4. Behavior of the rail under the condition applied the inter story drift

The behavior of the rails in this experiment is inferred from the strain gauges attached to the rails. Strain gauges were attached to the back side (a, b) and rail side (c, d) of each rail (loading jack side (S-side) and on the opposite side (N-side)) at three locations at the cross-sectional height. Figure 5(b) shows the distribution of the average strain on the back side and the average strain on the rail side, assuming plane retention. The vertical axis is the average strain value, and the strain distribution was at most 200 μST even when a maximum story drift angle of about 6% is introduced. That means the rails are elastic because each of the strain does not reach to yield strain (approximately 235/206000 ≈ 1140.7...μST for 400N class steel). Figures 5(a) and 5(c) show the strain distribution at the backside of each rail in the height direction. In Chapter 4, we will analyze the strain distribution on the N side when the story drift angle of 1%, which is assumed in the design, as introduced in the experiment.

The strain of the rail near the lower guide shoe on the S side was the largest, and the strain near the upper guide shoe on the N side was also large. Although the deformation of the counterweight due to the story drift angle was almost negligible, the deformation of the guide rails would have been occurred because of the contact with the counterweight through the guide shoes.

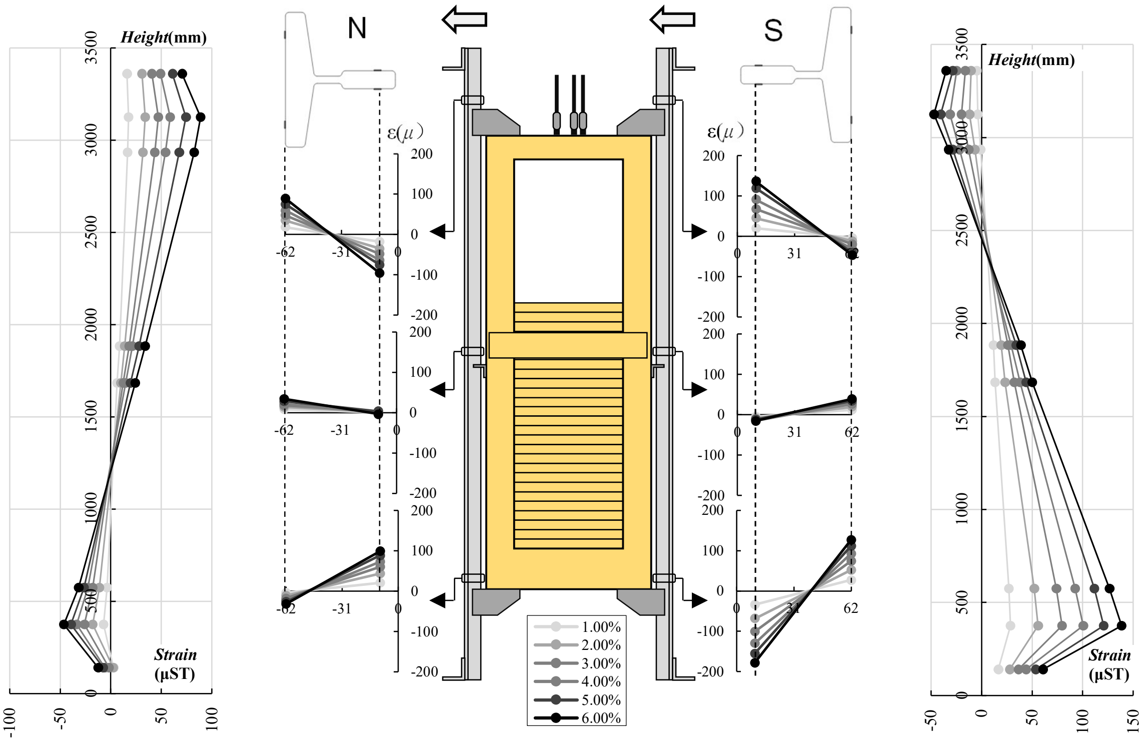

(a) N-side (b) section (c) S-side

Figure 5. Strain distribution of the rails

4. TRIAL OF THE VERIFICATION BASED ON THE BSL IN JAPAN

4.1. Analysis Model Conditions and Calculation Procedure

The experimental results confirmed that the strain occurs in the rails even when only the story drift angle was applied. In this section, we examine to predict the effect of story drift angle for the rails using simple mechanical model.

Figure 6 shows the analysis models of one rail.

The simple analytical model for the condition of being subjected to a two-point concentrated load from a position corresponding to the upper and lower shoe on the counterweight section with the story drift angle acting is assumed to be the fixed beam model (see Figure 6(b)) and the supported beam model (see Firgure 6(c)). The strain of the rail is obtained by following calculations:

(i) Calculate the bending moment due to the story drift angle, M1(x), and the bending moment due to two-point concentrated loads, M2(x), respectively.

(ii) To obtain the total bending moment: M0(x)=M1(x)+M2(x).

(iii) Obtain the bending stress: $\sigma 0(x) = M0(x)/Z$ from the total bending moment in (ii).

(iv) Solve the differential equation of deflection: $y0''(x) = \dfrac{-M0(x)}{E \cdot I}$ from the total bending moment in (ii) to obtain the amount of deflection y0(x).

(v) Obtain the deflection y3(x) in the same way as (i) ~ (iv) for the fixed beam model. In the supported beam model, bending moment due to the story drift angle, M1(x), is zero.

(vi) Calculate the strain: ε(x) of the analytical model by σ(x)=ε(x)·E from the stress of the analysis model obtained in (iii), where Z: section modulus of guide rail, I: moment of inertia of guide rail section, E: Young's modulus, 206000N/mm2.

4.2. Analytical result

Since both the N-side (north side) and S-side (south side) move almost equivalently, the N-side guide rail is targeted and verified for the story drift angle of 1%, which is close to the limit of the guaranteed area (about 0.83%) according to the law.

The loading conditions for the upper and lower guide shoes are shown in the table below. The load distribution between the upper and lower sections is 40% for the upper section and 60% for the lower section, which is the same as the current regulatory standard. Strain distributions for each analytical model and experimental result are shown in Figure 6(a).

Table 1. Assumption of the analyses

The story drift angle: R (%)	Weight load (N)	Upper-and lower-part load (N)	Upper load: R1(N)	Lower load: R2(N)
1.0	10780	107.8	43.1	64.7

4.3 Discussion of the results

Comparison of the calculated results and experimental results represents some findings as follows:

(i) The result of the fixed beam model and the experiment result show a similar trend for the gradient of the strain distribution. However, the model cannot reproduce the experiment result, which means that the boundary condition of the end of the actual rail is not so fixed.

(ii) In the supported beam model, the gradient of the strain distribution differs from that of the experiment result. That is presumably because the model is not included the effect of the story drift angle in.

The results above suggest that the influence of the story drift angle may be underestimated during seismic design if the model is based on the supported beam model.

In the experiment, the gap between the guide shoe and rail of the specimen was less than the allowable value. When the story drift angle is applied under these conditions, not only the force of the upper and lower shoes pushing the rails but also the force of the shoes gripping the rails is generated, which may have caused an inversion of the strain distribution.

Considering the above problems, Figure 6(a) also shows the strain distribution by the analytical model with the story drift angle adjusted to 1% and the concentrated load adjusted to 110N at the top and 45N at the bottom, as shown in Figure 6(d). The result can reproduce the experimental strain distribution, but the model is not a method that can be predicted in seismic design of the elevator. Therefore, a simple method to take the effect of the story drift into account in the seismic design is proposed.

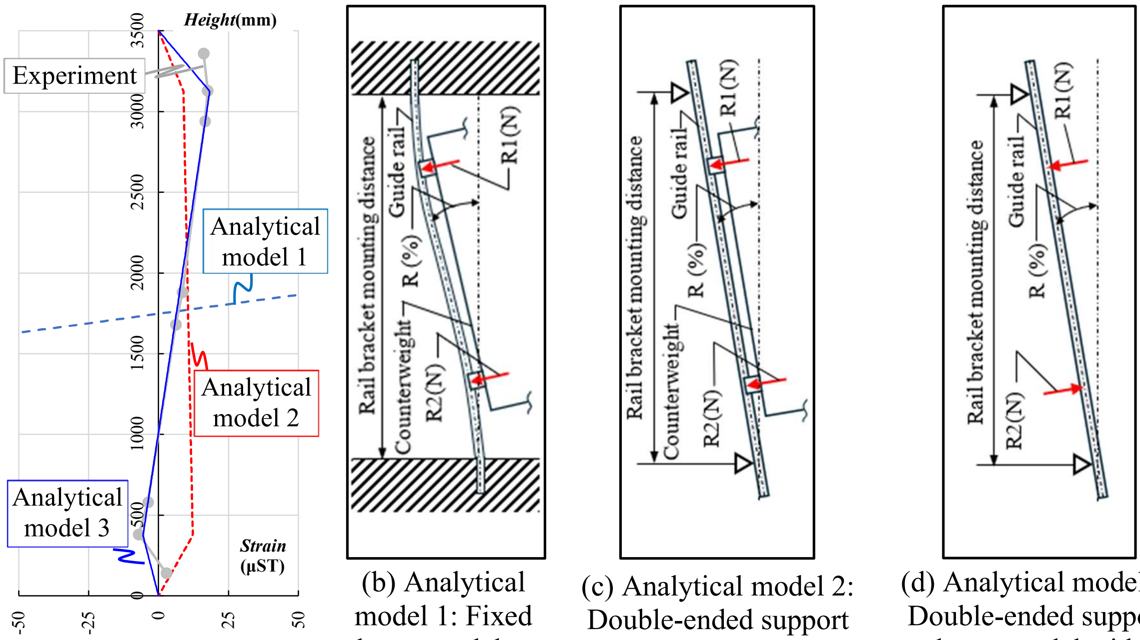

(a) Strain distribution (R≈1%)

(b) Analytical model 1: Fixed beam model at both ends.

(c) Analytical model 2: Double-ended support beam model with concentrate load due to counterweight based on [1]

(d) Analytical model 3: Double-ended support beam model with adjusted concentrate load condition due to counterweight.

Figure 6. Strain of the N-side rail (comparison of the results of the experiment with analyses)

4.4 Suggestion for seismic design based on the current regulations

The maximum values of the strain generated in the rails are listed below in comparison with the values converted as shown in Section 4.1 from the calculation results based on the current regulations introduced in Chapter 2, and the maximum values of the strain from the experimental results.

Table 2 shows the strain converted from the equations introduced in Chapter 2 as shown in Section 4.1 and the maximum strain distribution in the experimental results.

Table 2. The strain calculated from the BSL and the section 4.2, experimental data

The story drift angle:1%	Max. strain (μST)	Remarks
Experimental data	28.44	Lower load point on S-side (south side)
Building height 60m or less	14.50	
Building height over 60m	163.41	

From the Table 2, if the calculations are performed as in the formula for building heights over 60m, the values can be evaluated to be larger than those obtained experimental result where only the story drift angle is applied. In other words, it is recommended that the calculation can be performed in the same manner as the equation for the case of more than 60 m in the current regulations, in order to assume the influence of the story drift angle.

5. CONCLUSION

This paper firstly reviews the methods of elevator rails under current regulations for the seismic design of elevators. In the review, it showed that the current regulations except for the case of over 60m height do not consider the effect of the story drift angle of the building, in the method of verifying the stress and deflection of the rails.

To consider the effect of the story drift angle, an experiment around the counterweight (included rails) is presented. Experimental results show that only application of the story drift angle causes strain in the rails. We examined whether the experimental results could be reproduced by simple analytical models.

Based on the comparison of experimental and the analytical results, it is recommended that the calculation can be performed in the same manner as the equation for the case of more than 60 m in the current regulations, in order to assume the influence of the story drift angle.

Although this experiment was conducted only in one direction of the guideway, we would like to conduct experiments in another direction as well to further improve the accuracy of the verification.

ACKNOWLEGEMENTS

The support of the National Institute of Land and Infrastructure Management, the Building Research Institute, and all those involved in the Ministry of Land, Infrastructure, Transport and Tourism's comprehensive technical development project is gratefully acknowledged.

REFERENCES

[1] Commentary on Technical Standards for Elevators and Escalators, 2016 Edition

[2] FY2022 Building Standards Development Promotion Project P14 "Study report on preventing elevator entrapment during earthquakes"

[3] Minister's certificate: MSTL-0440 (Guide rail: T75/B)